Inorganic Chemistry

ARTICLE

pubs.acs.org/IC

Synthesis and Characterization of Thorium(IV) Sulfates

Karah E. Knope, Richard E. Wilson, S. Skanthakumar, and L. Soderholm*

Chemical Sciences and Engineering Division, Argonne National Laboratory, Argonne, Illinois 60439, United States

Supporting Information

ABSTRACT: Three Th(IV) sulfates, two new and one previously reported, have been synthesized from aqueous solution. In all of the compounds, the sulfate anions coordinate the Th^{4+} metal center(s) in a monodentate manner with Th−S distances of 3.7−3.8 Å. $Th(SO_4)_2(H_2O)_7\cdot 2(H_2O)$ (**1**; $P2_1/m$, a = 7.224(1) Å, b = 12.151(1) Å, c = 7.989(1) Å, ss =98.289(2)°) and $Th_4(SO_4)_7(H_2O)_7(OH)_2\cdot H_2O$ (**2**; *Pnma*, a = 18.139(2) Å, b = 11.173(1) Å, c = 14.391(2) Å) each contain 9-coordinate monomeric (**1**,**2**) and dimeric (**2**) Th(IV) cations in monocapped square antiprism geometry. Alternatively, $Th(OH)_2SO_4$ (**3**; *Pnma*, a = 11.684(1) Å, b = 6.047(1) Å, c = 7.047(1) Å) is built from chains of hydroxo-bridged, 8-coordinate Th^{4+} centers. Whereas **1** adopts a molecular structure, **2** and **3** both exhibit 3D architectures. Differences in the dimensionality and the topology of **1**−**3** are manifested in the local coordination environment about the Th(IV) centers, the formation of oligomeric Th^{4+} species, and the extended connectivity of the sulfate ligands. Herein, we report the syntheses and characterization of **1**−**3** as well as the atomic correlations of **1** in solution, as determined by high-energy X-ray scattering (HEXS).

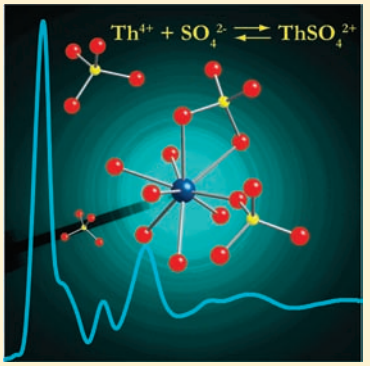

INTRODUCTION

The early actinides, unlike the early lanthanides, possess a number of oxidation states and chemistry similar to their transition metal homologues, an observation that initially frustrated the placement of the actinide series in the periodic table.[1,2] The early actinides Th through Pu exhibit a stable tetravalent oxidation state[3] and trends within their chemical behavior can generally be ascribed to the systematic decrease in ionic radii across the series.[4,5] These small changes in ionic radii can dramatically impact the coordination chemistry of these tetravalent ions in solution and the effects can be quantified in the metal cations' hydration states, hydrolysis behavior, and tendency to form inner- and outer-sphere interactions. The acidity and complex forming tendency generally decreases in the order Pu(IV) > Np(IV) > U(IV) > Th(IV), and the stability constants for many M(IV)−ligand systems highlight this trend, as shown by the An(IV) nitrates.[6−8]

M(IV) sulfate complexes in aqueous solution also follow the trend mentioned above, where Th is the weakest complex former.[6−8] Equilibrium constant values for the reaction $M(IV) + HSO_4^- \leftrightharpoons MSO_4^{2+} + H^+$ are 4.91, 4.87, 4.6, and 4.19 for Pu(IV), Np(IV), U(IV), and Th(IV), respectively. In a series of recent articles, Hennig et al. explored the structural chemistry of the tetravalent actinides with sulfate in aqueous solution and found a change in the distribution of the sulfate coordination mode with respect to the An(IV) ion.[9−11] Monodentate sulfate linkages were predominately observed for Th, whereas bidentate sulfate complexation was more favorable for the later actinides.[9] This phenomenon cannot be extrapolated from inspection of the stability constants. Surprisingly, little is known about An(IV)−sulfates systems. Unlike simple ligand systems such as the halides, sulfate provides a multitude of metal ion coordination modes and sulfuric acid (a diprotic acid), allows for an indirect probing of the effects of metal ion acidity and polarization on these coordination modes (i.e., monodentate HSO_4^- versus mono or bidentate SO_4^{2-}).

Recently, Wilson demonstrated limited correlation among the tetravalent actinides, Ce(IV), and the group IV metals in a study of the solid-state chemistry of the Pu(IV) sulfates.[12] The nine structures reported for the softest member of the tetravalent ions, Th(IV),[13−20] showed very little structural similarity in the solid state with any of the other tetravalent cations in the periodic table. In fact, there is only one actinide sulfate, $M(OH)_2SO_4$, for which Th, U, and Np form an isomorphic series.[19,21,22] The chemical reasons for this are unclear and motivate this study.

Thorium is the largest, chemically softest, and least polarizing of the tetravalent metal ions.[23] Relative to the other tetravalent cations, Th is least likely to undergo hydrolysis and complex formation for a given ligand. These chemical properties of thorium allowed for the isolation of the homoleptic deca-aqua complex, to date the only homoleptic aqua complex of a tetravalent ion.[24] Using thorium, the end member of this periodic group of tetravalent metal ions, can we identify and correlate the periodic solution state behavior and structures observed in the An(IV) sulfates with that observed in the solid state, and with the remainder of the M(IV) sulfates? Toward this goal, we have synthesized a series of thorium sulfate compounds described herein. In an effort to inform current and future synthetic strategies, we used high-energy X-ray scattering (HEXS) to ascertain and quantify

Received: May 31, 2011
Published: August 03, 2011

metal−metal, metal−solute, and metal−solvent correlations in the solution from which crystals of **1** formed.

Coupled herein are the syntheses of three thorium sulfates, their solid-state structural characterization,[19,25] and the Th speciation in one of the solution preparations. These compounds all exhibit exclusively monodentate sulfate linkages yet $Th(SO_4)_2(H_2O)_7\cdot 2(H_2O)$ (**1**) adopts a molecular structure in which the SO_4^{2-} ligands are terminal whereas $Th_4(SO_4)_7(H_2O)_7(OH)_2\cdot H_2O$ (**2**) and $Th(OH)_2SO_4$ (**3**) adopt higher dimensional structures due to the bridging nature of the SO_4^{2-} unit. The SO_4^{2-} coordination in a solution prior to crystallization of **1** reveals the presence of both monodentate and bidentate Th ligation as well as evidence for sulfate bridging two Th, a bonding motif seen in the solid state.

EXPERIMENTAL METHODS

Synthesis. *Caution: ^{232}Th is an alpha-emitting radionuclide and standard precautions for handling radioactive materials should be followed when working with the quantities used in the syntheses that follow.*

Compound **1**, $Th(SO_4)_2(H_2O)_7\cdot 2(H_2O)$, was synthesized at room temperature from the reaction of $Th(ClO_4)_4\cdot nH_2O$ (100uL of a 2.69 M solution, 0.26 mmol) and concentrated H_2SO_4 (0.0139 mL, 0.26 mmol) in 0.463 mL of distilled water. Colorless crystals formed after several days. Compound **1** can be synthesized after a few hours by increasing the sulfate concentration. For example, crystals of **1** can be prepared from the room temperature reaction of $Th(ClO_4)_4\cdot nH_2O$ (100uL of a 2.69 M solution, 0.26 mmol) and concentrated H_2SO_4 (0.027 mL, 0.52 mmol) in 0.463 mL of distilled water. Upon addition of H_2SO_4 to the $Th(ClO_4)_4$ solution a white precipitate is formed. The precipitate redissolves and crystals of **1** can be isolated after a few hours. FTIR: 3420 (O−H), 1660 (H−O−$H_{bending}$), 1110 (O−SO_3), 1050 (O−SO_3), 992 (O−SO_3), and 606 cm^{-1}. Raman: 1137, 1047, 1007, 619, 445, 387, 332, 265, 245, 219, 178, 153, and 123 cm^{-1}.

Compound **2**, $Th_4(SO_4)_7(H_2O)_7(OH)_2\cdot H_2O$, was synthesized hydrothermally. Amorphous $Th(OH)_4$ was precipitated with NH_4OH from a 1 mL solution of 0.1 M $Th(NO_3)_4$ in H_2O. The resulting white precipitate was washed several times with distilled water until the pH of the supernatant was near neutral. The pellet was dissolved in 0.25 M H_2SO_4 (1 mL, 0.25 mmol) and transferred to a 3 mL Teflon linear that was placed in a 45 mL Teflon lined Parr bomb. The reaction vessel was backfilled with 5 mL of H_2O, sealed and then heated statically at 180 °C. After 6 days, the reaction was removed from the oven and cooled to room temperature over 4 h. Clear, colorless plates were obtained. Yield: 57% based on thorium. FTIR: 3390 (O−H), 1660 (H−O−$H_{bending}$), 1100 (O−SO_3), and 595 cm^{-1}. Raman: 1232, 1188, 1115, 1102, 1065, 1054, 1027, 651, 630, 608, 456, 350, 321, 241, 227, 203, 188, 162, 151, 141, and 123 cm^{-1}.

Compound **3**, $Th(OH)_2SO_4$, was prepared from the hydrothermal reaction of 0.1 M $Th(NO_3)_4$ (0.5 mL, 0.05 mmol) and 0.5 M H_2SO_4 (0.5 mL, 0.25 mmol). The reactants were added to a 3 mL Teflon cup that was placed into a 45 mL Teflon lined Parr bomb. The reaction vessel was backfilled with 5 mL of H_2O, sealed and then heated statically at 180 °C for 6 days. Colorless plates were obtained after cooling the reaction to room temperature. Yield: 63% based on thorium. FTIR: 3570 (O−$H_{bridging}$), 3370 (O−H), 1660 (H−O−$H_{bending}$), 1110 (O−SO_3), 764 and 585 cm^{-1}. Raman: 1182, 1146, 1131, 1098, 1081, 1042, 852, 813, 741, 647, 626, 609, 474, 463, 449, 381, 343, 223, 183, 156, 144, and 123 cm^{-1}.

X-ray Structure Determination. Reflections were collected at 100 K on a Bruker AXS SMART diffractometer equipped with an APEXII CCD detector using Mo Kα radiation. The data were integrated and corrected for absorption using the *APEX2* suite of crystallographic software.[26] All structures were solved using direct methods and refined using *SHELXL-97*.[27] Satisfactory refinements as well as tests for missing symmetry, using Platon,[28] indicated that no obvious space group changes were needed or suggested. Crystallographic data for **1**−**3** are provided in Table 1 and CIF data are available as Supporting Information.

Table 1. Crystallographic Data and Structure Refinement for 1−3

	1	2	3
formula	$H_{18}O_{17}S_2Th$	$H_{18}O_{38}S_7Th_4$	H_2O_6STh
MW	586.30	1778.72	362.12
temperature (K)	100	100	100
λ (Mo Kα)	0.71073	0.71073	0.71073
cryst syst	monoclinic	orthorhombic	orthorhombic
space group	$P2_1/m$	*Pnma*	*Pnma*
a	7.2244(9)	18.1390(20)	11.6838(10)
b	12.1506(14)	11.1729(14)	6.0470(5)
c	7.9889(9)	14.3913(19)	7.0471(6)
α	90	90	90
β	98.289(2)	90	90
γ	90	90	90
V	693.95(14)	2916.7(7)	497.89(7)
Z	2	4	4
D_{calcd} (g cm^{-3})	2.806	4.051	4.831
μ (mm^{-1})	11.133	20.979	30.310
$R_1{}^a$ [$I > 2\sigma(I)$]	0.0305	0.0328	0.0192
$wR_2{}^a$	0.0620	0.0777	0.0458

$^a R_1 = \Sigma||F_o| - |F_c||/\Sigma|F_o|$; $wR_2 = \{\Sigma[w(F_o^2 - F_c^2)^2]/\Sigma[w(F_o^2)^2]\}^{1/2}$.

All non-hydrogen atoms were located using difference Fourier maps and were ultimately refined anisotropically. Hydrogen atoms of the bound water molecules in **1** were found during refinement. Whereas the hydrogen atoms of O1−O3 were freely refined, those of O4 and O5 were refined with O−H distance restraints of 0.82 Å. Hydrogen atoms of the solvent water were located in the difference Fourier map however their assignment did not support a satisfactory refinement. Similarly, hydrogen atoms of the bridging hydroxide groups (O2−O3) were located in the structure of **2** but assignment did not support a satisfactory refinement. Hydrogen atoms of the bound and solvent water molecules were not found. Additionally, hydrogen atoms of the bridging water molecule (O4) were not found but a lengthened Th−O bond distance of 2.678(7) Å as well as bond valence values[29] are consistent with our assignment of O4 as a water molecule. The hydrogen atom of the hydroxide group (O4) in **3** was located and refined with a distance restraint of 0.82 Å.

Powder X-ray diffraction data were collected for **1**−**3** using a Scintag X1 diffractometer (Cu Kα, 3−40°). Rietveld refinement of the powder patterns was performed using EXPGUI,[30] a user interface to GSAS,[31] wherein the initial structure parameters were those obtained from single crystal data. Agreement between the calculated and observed patterns (Figures SI4−SI6 of the Supporting Information) confirms that the single crystals used for structure determination were representative of the bulk sample.

High-Energy X-ray Scattering (HEXS). High-energy X-ray scattering data of the 1:1 Th:SO_4 solution from which **1** was prepared (prior to crystallization) were collected at the Advanced Photon Source (APS), Argonne National Laboratory on beamline 11-ID-B. Background solutions, containing no Th^{4+} were also prepared so that only Th correlations remained after subtraction of the scattering data from the background solution from that of the solution from which **1** was isolated. The incident beam of 91 keV corresponds to a wavelength of 0.13702 Å.

dx.doi.org/10.1021/ic201175u |*Inorg. Chem.* 2011, 50, 8621–8629

Table 2. Selected Distances and Angles.[a]

		1	
Th(1)−O(1)	2.504(5)	Th(1)−S(1)	3.793(1)
Th(1)−O(2)	2.477(5)	O(1)−H(1A)···O7^{i}	2.778(5)
Th(1)−O(3)	2.468(3)	O(2)−H(2)···O7^{ii}	2.740(5)
Th(1)−O(4)	2.485(3)	O(3)−H(3A)···O9^{ii}	2.722(5)
Th(1)−O(5)	2.439(4)	O(3)−H(3B)···O9^{iii}	2.768(5)
Th(1)−O(6)	2.379(3)	O(5)−H(5A)···OW1	2.658(6)
O(6)−S(1)	1.482(3)	Th(1)−O(6)−S(1)	157.67°
O(7)−S(1)	1.474(3)		
O(8)−S(1)	1.467(3)		
		2	
Th(1)−O(1)	2.472(5)	Th(3)−O(13)	2.357(5)
Th(1)−O(2)	2.391(4)	Th(3)−O(17)	2.573(8)
Th(1)−O(3)	2.357(5)	Th(3)−S(3)	3.726(2)
Th(1)−O(4)	2.678(6)	S(1)−O(7)	1.476(5)
Th(1)−O(7)	2.456(5)	S(2)−O(13)	1.461(5)
Th(1)−Th(1)	3.884(1)	S(2)−O(14)	1.473(5)
Th(1)−S(1)	3.770(1)	S(3)−O(19)	1.477(5)
Th(1)−S(2)	3.834(1)	S(3)−O(21)	1.451(5)
Th(2)−O(10)	2.380(7)	S(4)−O(8)	1.464(5)
Th(2)−O(16)	2.596(7)	Th(1)−O(7)−S(1)	145.83°
Th(2)−S(1)	3.861(2)	Th(2)−O(10)−S(1)	175.48°
		3	
Th(1)−O(1)	2.462(3)	Th(1)−S(1)	3.707(1)
Th(1)−O(2)	2.453(3)	Th(1)−S(1)^{vi}	3.786(1)
Th(1)−O(3)	2.467(4)	S(1)−O(1)	1.463(4)
Th(1)−O(4)	2.348(3)	Th(1)−Th(1)^{iv}	3.967(1)
Th(1)-O4^{iv}	2.356(3)	Th(1)−O(1)−S(1)	140.22°

[a] Superscript denotes symmetry transformations (**1**) $i = -x + 2, -y, -z + 1$; ii = $-x + 2, -y, -z + 2$; iii = $x - 1, y, z$ (**3**) iv = $-x, -y, -z$; vi = $-x, -y, -z + 1$.

Samples were loaded in Kapton capillaries with epoxy plugs and further contained as required for actinide samples. Scattered intensity was measured using an amorphous silicon flat panel X-ray detector mounted in a static position ($2\theta = 0°$) providing detection in momentum transfer space Q (Å^{-1}) up to 32 Å^{-1}. Data were treated as described previously.[32,33]

IR and Raman Spectroscopy. IR spectra were collected on a Nicolet Nexus 870 FTIR system. The samples were diluted with dried KBr and pressed into a pellet. Scans were collected over 4000−400 cm^{-1} with 64 scans and 2 cm^{-1} resolution. Raman spectra of powder samples of **1**−**3** were collected on a Renishaw inVia Raman Microscope with an excitation line of 532 nm.

RESULTS

Structure Descriptions. Compounds **1**−**3** all contain sulfate groups that coordinate each individual Th^{4+} center in a monodentate manner.[19,25] Differences in dimensionality and topology, however, are observed in **1**−**3** due to variation in the coordination environment about the Th(IV) centers as well as the coordination behavior of the sulfate anions. Selected bond distances and angles are listed in Table 2.

Compound **1**, $Th(SO_4)_2(H_2O)_7 \cdot 2H_2O$, adopts a molecular structure, shown in Figure 1, that is built from one crystallographically unique thorium(IV) metal center, one unique SO_4^{2-} group and six crystallographically unique water molecules (O1−O5 and OW1). Overall, Th(1) exhibits a monocapped square antiprism geometry resulting from its coordination to nine oxygen atoms from seven bound water molecules and two monodentate sulfate anions. Sulfate oxygen atoms O7−O9 remain unbound, thus limiting dimensionality. The average thorium−oxygen bond distances for coordinated water molecules and monodentate sulfate groups are 2.468 Å and 2.379 Å, respectively. The Th−O−S bond angle of 157.7° and a Th−S distance of 3.79 Å are consistent with other Th−SO_4 structures containing monodentate sulfate linkages.[13,16] As depicted in Figure 2, hydrogen bonding interactions between the bound water molecules O1, O2, and O4 and distant sulfate oxygen atoms from adjacent $Th(H_2O)_7(SO_4)_2$ units are present in structure of **1**; O−H···O distances range from 2.722 to 2.768 Å. Also highlighted in Figure 2 are correlations between thorium and four sulfur atoms from distant thorium bound sulfate ligands which occur at 5.336−5.349 Å.

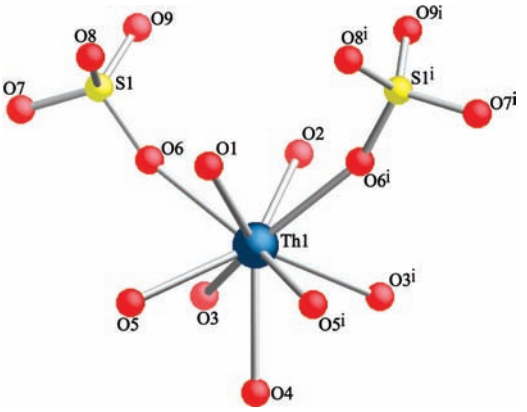

Figure 1. Illustration of **1** showing the local coordination environment of Th(1). Hydrogen atoms have been omitted for clarity. Superscript denotes symmetry transformations $i = x, -y + {}^{1}/_{2}, z$.

Compound **2**, $Th_4(SO_4)_7(H_2O)_7(OH)_2 \cdot H_2O$, adopts a 3D architecture. As shown in Figure 3, sheets of sulfate bridged ThO_9 monomers (bolded in black and highlighted in part a of Figure 4) are connected along [100], via bridging SO_4^{2-} units, to chains of sulfate linked Th_2O_{15} dimers (bolded in red) that extend infinitely along [010] (parts b and c of Figure 4). The structure is built from three crystallographically unique Th(IV) metal centers and four unique SO_4^{2-} units. Each of the Th(IV) metal centers exhibits monocapped square antiprism geometry. Sulfate units S(1)O_4 and S(4)O_4 are coordinatively saturated, whereas S(2)O4 and S(3)O4 each have one oxygen atom (O14 and O21, respectively) that remains unbound. Th(2) and Th(3) are each coordinated to 9 oxygen atoms from seven monodentate sulfate ligands and two bound water molecules to form Th-$(SO_4)_7(H_2O)_2$ units. These monomers are connected via sulfate linkages into 2D sheets highlighted in part a of Figure 4. Alternatively, Th(1) is bound to nine oxygen atoms from five monodentate sulfate anions, two hydroxide groups (O2 and O3), one bound water molecule (O1) and one bridging water molecule (O4) at distances of 2.395−2.473 Å, 2.358−2.392 Å, 2.478 Å and 2.678 Å, respectively. A rare linkage (part c of Figure 4) consisting of hydroxide oxygen atoms O2 and O3 and one water molecule, O4, bridges two Th(1) cations into face sharing dimers (parts b and c of Figure 4) that have Th(1)−Th(1) distances of

dx.doi.org/10.1021/ic201175u |*Inorg. Chem.* 2011, 50, 8621–8629

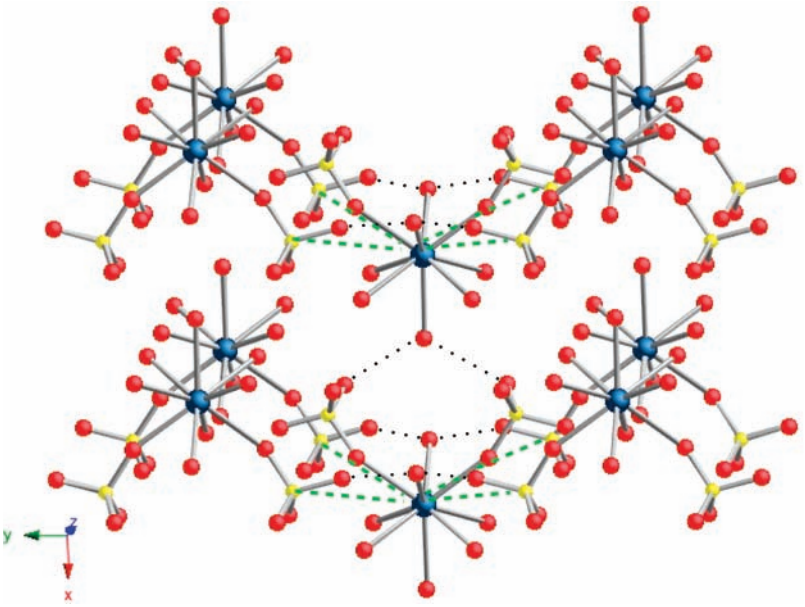

Figure 2. Packing diagram of **1** highlighting the hydrogen bonding interactions (black dotted lines) between oxygen atoms of the bound water molecules and the unbound sulfate oxygen atoms from adjacent $Th(H_2O)_7(SO_4)_2$ units. Also shown (green dashed lines) are the correlations between Th and the sulfur atoms of distant sulfate ligands.

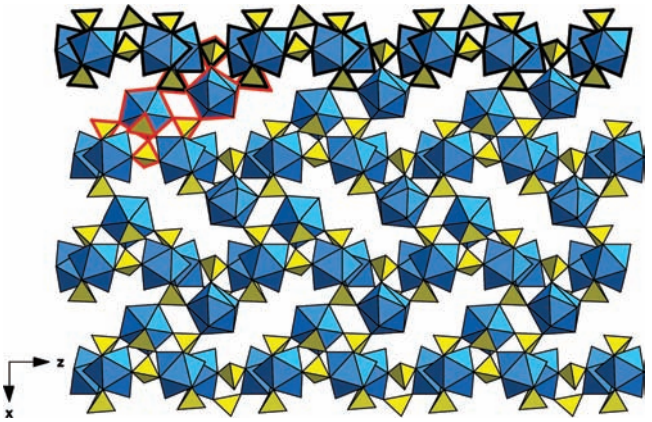

Figure 3. Polyhedral representation of **2** viewed down the [010] direction. 2D sheets (bolded in black) of sulfate bridged Th(2) and Th(3) monomers are connected along [100], via SO_4^{2-} units, to chains of sulfate linked Th(1)−Th(1) dimers (bolded in red). Bolded sections are highlighted in Figure 4. Blue polyhedra are Th(IV) in monocapped square antiprism geometry and yellow polyhedra represent SO_4^{2-} anions. Solvent water molecules have been omitted for clarity.

3.884 Å. The Th−O bond distances of the bridging hydroxide are significantly shorter (2.357−2.391 Å) than that of the bridging water molecule (2.678 Å). As illustrated in part b of Figure 4, $S(1)O_4^{2-}$ units link the resulting dimers into chains that run along [010]. Each $S(1)O_4^{2-}$ group additionally coordinates one Th(2) and one Th(3) metal center thereby linking the Th(1) dimers to the sheets of sulfate bridged Th(2)O9 and Th(3)O9 monomers described above (part a of Figure 4). The dimers are additionally connected to the sheets via sulfate groups S(2)O4−S(4)O4.

Compound **3**, $Th(OH)_2SO_4$, has been previously reported by Lundgren,[19] but for the purposes of discussion a brief description is given. As shown in Figure 5, the structure is built from $[Th(OH)_2]_n^{2n+}$ chains that extend infinitely down [010]. The chains are further connected via sulfate linkages along [100] and [001] into a 3D architecture (Figure 6). The Th(IV) center adopts a square antiprism coordination geometry as it is coordinated to four hydroxide oxygen atoms (O4 and its symmetry equivalents) and four oxygen atoms from four monodentate sulfate ligands. Th−O(H) and Th−O(SO_3) bond distances range from 2.348 to 2.356 Å and 2.453−2.467 Å, respectively. The Th−Th distance within the hydroxo bridged units is 3.967 Å.

IR and Raman Spectroscopy. The IR spectra of **1**−**3** (Figures S7−S9 of the Supporting Information) show bands consistent with metal-bound sulfate ligands with stretches appearing around 1100 cm^{-1}.[34] The peaks at 3400 cm^{-1} and 1660 cm^{-1} are indicative of −OH in H_2O. Additionally, the peak at 3570 cm^{-1} in the spectrum of **3** is consistent with a bridging −OH.[22,34] The Raman spectra (Figures S10−S12 of the Supporting Information) are similarly indicative of thorium bound sulfate with strong bands centered at approximately 1100−1050 cm^{-1}, and weaker bands appearing at 650 cm^{-1} and 450 cm^{-1}.[20]

High Energy X-ray Scattering. The Fourier transformed (FT) HEXS data obtained from a solution containing 0.5 m $Th(ClO_4)_4$ and 0.5 m SO_4^{2-}, after subtraction of solvent−solvent interactions, are presented in Figure 7. Crystals of $Th(SO_4)_2(H_2O)_7 \cdot 2(H_2O)$ (**1**) form from these solutions upon standing. The sulfate data are compared in the figure with HEXS data from the Th homoleptic aqua ion in dilute $HBr/HClO_4$.[24] As previously described, peaks in the FT were fit with Gaussians to quantify Th solution correlations,[35] a summary of which is provided in Table 3. Although the two patterns are similar, in addition to the peaks seen in the Th aqua ion PDF, notable correlations are also observed in the sulfate data at 3.19(5) Å, 3.75(3) Å, and 5.9(2) Å.

The first peak in the thorium sulfate patterns, centered at 2.47(2) Å, is attributed to Th correlated to nine oxygen atoms. This solution coordination compares with a previous HEXS

dx.doi.org/10.1021/ic201175u |*Inorg. Chem.* 2011, 50, 8621–8629

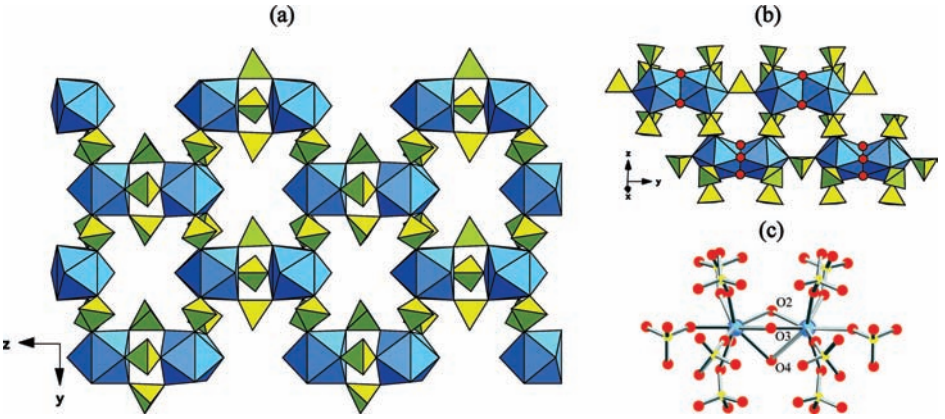

Figure 4. Illustration of **2** showing the (a) topology of the 2D sheets that are built from $Th(2)O_9$ and $Th(3)O_9$ polyhedra connected via sulfate linkages, (b) chains of Th_2O_{15} dimers linked along [010] by $S(1)O_4^{2-}$ units, and (c) local structure of the Th(1)−Th(1) dimers. Blue polyhedra are Th(IV) in monocapped square antiprism geometry and yellow polyhedra represent SO_4^{2-} anions. Blue, yellow and red spheres represent Th^{4+}, sulfur, and oxygen, respectively.

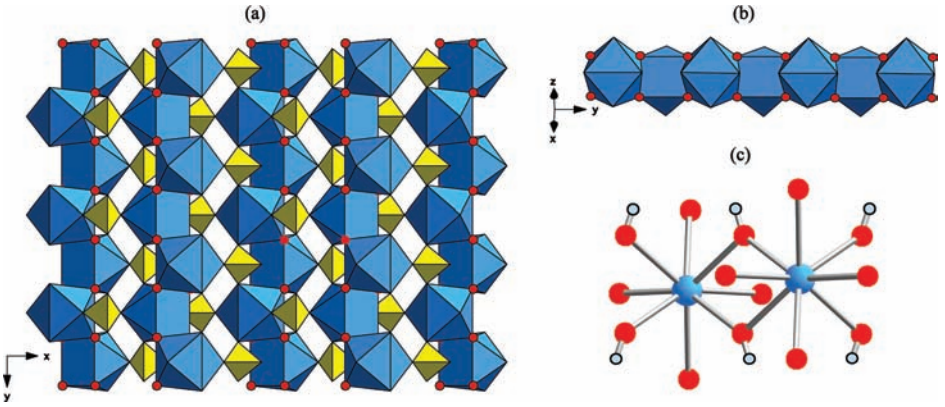

Figure 5. Illustration of **3** showing (a) zigzag chains of $[Th(OH)_2]_n^{2n+}$ that are connected by SO_4^{2-} units into an extended network, (b) a polyhedral representation of the hydroxo bridged $[Th(OH)_2]_n^{2n+}$ chains and (c) a ball and stick representation of the hydroxo bridged Th(IV) centers.

study of the aqua ion, which has 10.1(3) O at an average of 2.46(1) Å[24] and an EXAFS study that finds one O shell, with an average coordination number of 9.3(14) at 2.43 Å.[11] The Th−O weighted average from the single crystal structure is 2.448 Å, slightly shorter than the distance observed in solution.

Following previous precedent, the scattering tail to higher *r* of the Th−O peak in the PDF is attributed, at least in part, to the H atoms associated with the first coordination sphere waters.[36,37] In this case the scattering tail is represented by two Gaussians with positions that refine to 2.91(4) Å and 3.19(4) Å, as depicted in Figure 8. Because of the difficulty in resolving the scattering intensities from these two peaks, their intensities are summed for assignment. Taking guidance from the X-ray structure, there would be 14 H atoms assigned to this peak, based on the seven waters associated with Th in the solid state. Similar scattering from actinide coordinated waters has been previously observed.[24,36,37] The peak at 3.19(4) Å, which is not present in the aqua ion data, occurs at a distance consistent with Th−bidentate sulfate coordination in solution. This coordination mode does not occur in the solid state structure of **1**, in which only monodentate sulfate ligation is seen. The peak at 3.75(3) Å in the PDF is at a distance representative of Th−S correlations for monodentate sulfate coordination. For example, EXAFS studies of Th sulfate solutions find a Th−S interaction at 3.81(2) Å for monodentate sulfate ligation.[11] Expected in the same *r* region are the two Th−O correlations from the bidentate sulfate anion.

There is no evidence for the presence of water- or hydroxo-bridged Th−Th dimeric interactions, which would appear at about 3.9 Å in the FT of solution HEXS data.[38] The peak at 4.6 Å is at a similar distance to that seen for the Th homoleptic aqua ion, where it is attributed to second-coordination sphere waters.[24] However, the sulfate data appear to have less of a shoulder to higher *r* for this outer-sphere water peak and also have a much more defined peak even farther from the Th, at a distance of about 5.9 Å. Because these features are absent in sulfate-free Th solutions, including those containing perchlorate as a counterion, the scattering at 5.9 Å is attributed to either to an outer sphere Th−S correlation or a Th−Th correlation mitigated by a bridging sulfate. Th correlations to a second coordination sphere sulfate have been previously observed at 5.884 Å,[13] the connectivity involving a Th-bound water hydrogen bonding to a sulfate oxygen. Similar bonding connectivity occurs in compound **1**, where six sulfur atoms are located at a distance of 5.336−5.349 Å. A more likely contribution to the HEXS scattering peak at 5.9 Å would be a Th−Th interaction involving a bridging sulfate, similar to that seen in the crystal structure of

dx.doi.org/10.1021/ic201175u |*Inorg. Chem.* 2011, 50, 8621–8629

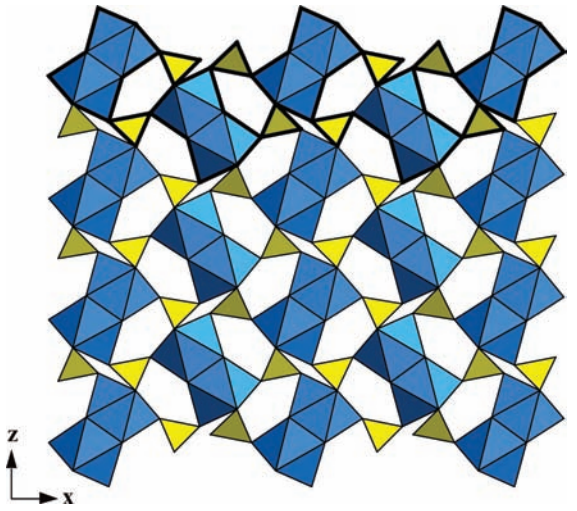

Figure 6. Polyhedral representation of **3** viewed down the [010] direction. Chains of hydroxide bridged ThO_8 units that run infinitely down [010] are linked via sulfate ligands along [100] and [001] into a 3D structure. The section bolded above is shown in part a of Figure 4.

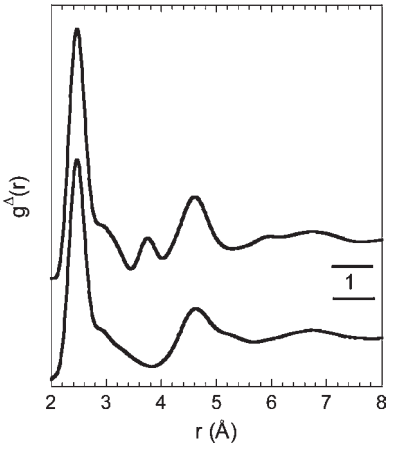

Figure 7. Fourier transformed high-energy X-ray scattering (HEXS) data from the solution that produced **1** (top) after subtraction of solvent−solvent interactions[33,35] compared with a solution pattern of the Th(IV) aqua ion (bottom).[24]

Table 3. Results of Fitting the Background Subtracted FT HEXS Data to a Series of Gaussians, As Shown in Figure *8*; Peak Assignments Are Discussed in the Text

peak position (Å)	electrons	assignment
2.47(2)	72(2)	9 oxygen
2.91(4)	23(4)	16 hydrogen+
3.19(4)	5.7(10)	∼0.8 sulfur
	101	102 total
3.75(3)	20(2)	2 oxygen + ∼0.2 S
4.6(1)	96(5)	11−12 oxygen/waters
5.9(2)	25(8)	∼0.2 Th + sulfur
6.7(2)	∼140	

$K_4Th(SO_4)_4(H_2O)_2$ at 5.884 Å.[13] Assigning an accurate electron count to the 5.9 Å peak is difficult but the intensity is consistent

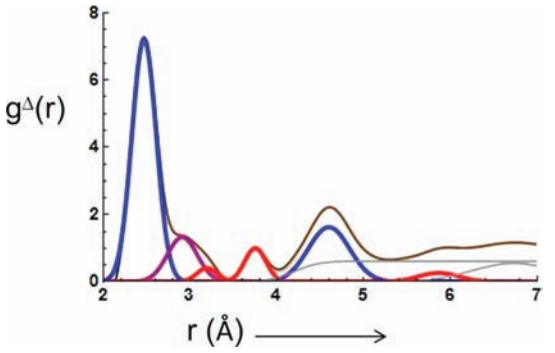

Figure 8. Fit (brown) of the PDF obtained from a solution of **1** after subtraction of solvent−solvent interactions. The peaks represent Th correlations with other solute and solvent ions. The pattern is fit with a series of Gaussians attributed to Th−O (blue), Th−H (purple), and Th−S, O, Th (red) as discussed in the text.

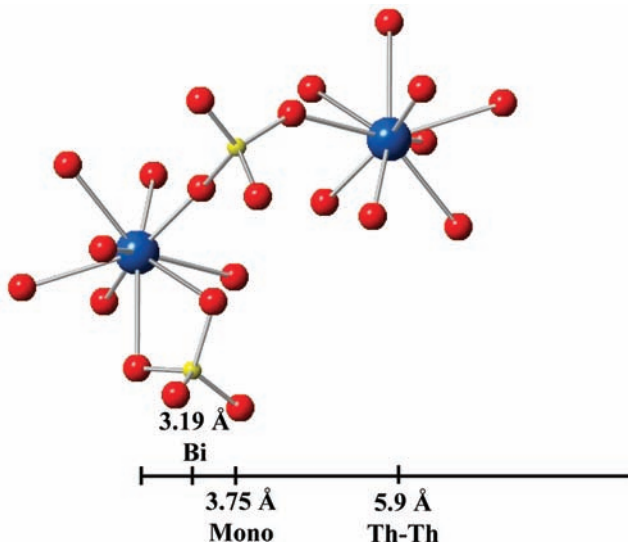

Figure 9. Illustration of the proposed types of Th correlations seen in solution. The Th (blue) is surrounded by nine O atoms (red) from water molecules, monodentate, and bidentate sulfate ions (sulfur, yellow). There is also a Th−Th interaction at 5.9 Å, consistent with that arising from a bridging sulfate group.[13]

with an average of at about 0.2 Th−Th bound in this fashion. The Th−S correlations observed at 3.19(5) Å, 3.75(3) Å and the Th−Th correlation at 5.9(2) Å proposed to result from monodentate, bidentate, and bridging sulfate respectively are illustrated in Figure 9.

The overall assignment of Th−S interactions, approximately 0.8 with bidentate coordination at 3.19(4) Å, about 0.2 monodentate (either bridging or not) at 3.75 Å, and a possible contribution to the peak at 5.9(2) Å are constrained by the Th:SO_4 ratio of 1:1 in solution. The HEXS data measure an average speciation in solution and therefore the total Th−S interactions cannot exceed this ratio. Interpreting this constraint is somewhat complicated by the possible inclusion of Th−Th and Th−S interactions observed at 5.9(2) Å, which would also contribute to other observed correlations. In the absence of a series of samples with varying Th:SO_4 ratios, the assignments of the PDF peaks remain somewhat uncertain. Such a series of data are precluded

dx.doi.org/10.1021/ic201175u |*Inorg. Chem.* 2011, 50, 8621–8629

Table 4. Summary of the Overall Coordination Number and Environment about the Metal Centers in Currently Known Th(IV) Sulfates[a]

compound	Th(IV) CN	N SO_4^{2-} Mono	N SO_4^{2-} Bi	N H_2O	N OH	ref
$Th(SO_4)_2(H_2O)_6 \cdot 2H_2O$	10	0	2	6	0	15
$Cs_2Th(SO_4)_3(H_2O)_2$	10	2	3	2	0	17
$[PIP][Th_3(SO_4)_6(H_2O)_6] \cdot H_2O$	10	5	2	1	0	18
	10	5	2	1	0	
	9	7	0	2	0	
$[DABCO]_2[Th_2(SO_4)_6(H_2O)_2] \cdot 2H_2O$	9	7	0	2	0	18
	9	6	0	3	0	
$K_4Th(SO_4)_4(H_2O)_2$	9	4	1	3	0	13
$Na_2Th(SO_4)_3(H_2O)_3 \cdot 3H_2O$	9	6	0	3	0	16
$Th_3(SO_4)_6(H_2O)_6 \cdot H_2O$	9	7	0	2	0	20
$Th(H_2O)_7(SO_4)_2 \cdot 2H_2O$	9	2	0	7	0	this work, 25
$Th_4(SO_4)_7(H_2O)_7(OH)_2 \cdot 2H_2O$	9	5	0	2	2	this work, 25
	9	7	0	2	0	
	9	7	0	2	0	
$Th(OH)_2(SO_4)$	8	4	0	0	4	19

[a] We note that $[Th(SO_4)_2(CH_4N_2O)_4(H_2O)] \cdot 2H_2O$ [14] has been omitted from the table as it contains urea ligands in the inner coordination sphere of Th(IV). PIP is piperazine and DABCO is 1,4-diazabicyclo[2.2.2]octane.

here because of the insolubility of Th−sulfates under the conditions necessary to obtain HEXS data.

DISCUSSION

The structures described here exhibit many features consistent with previously reported Th(IV) sulfates. The Th−O−S bond angles in **1**−**3** range from 140.22 to 175.48° and average 152.31°. Such values are typical for compounds containing monodentate coordinated sulfate groups. Alternatively, Th−O−S bond angles for chelating bidentate sulfate units such as those found in $Th(SO_4)_2 \cdot 8H_2O$[15] or $K_4[Th(SO_4)_4(H_2O)_2]$[13] average approximately 100°. Additionally the distribution of bond distances in **1**−**3** is comparable to that found in other Th(IV) sulfates. Thorium oxygen bond distances for monodentate coordinated sulfate and bound water molecules range from 2.357 to 2.473 Å and 2.438 to 2.505 Å, respectively.

The aqua ion, $[Th(H_2O)_{10}]Br_4$, contains ten water molecules in the first coordination sphere of Th^{4+}.[24] By comparison, as highlighted in Table 4, thorium(IV) sulfates show a distribution of metal ion coordination numbers with values ranging from 8 to 10. Interestingly, with the exception of $K_4Th(SO_4)_4(H_2O)_2$, bidentate sulfate coordination seems to be coincidental with higher coordination about the metal center. That is, Th(IV)−sulfate compounds that contain chelating sulfate units tend to form ten coordinate complexes. This is likely due to steric effects.

Compounds **1**−**3** contain sulfate units that bind each Th^{4+} center exclusively in a monodentate manner. Of the eight known thorium(IV) sulfates, three ($Na_2[Th(SO_4)_3(H_2O)_3] \cdot 3H_2O$,[16] $Th(OH)_2SO_4$,[19] and $Th_3(SO_4)_6(H_2O)_6 \cdot H_2O$[20] contain solely monodentate Th−SO_4 linkages. The remaining five compounds contain a combination of monodentate and bidentate coordination. In some cases, differences in metal−sulfate coordination modes have been attributed to sulfate/metal ratios. For example, Hennig and co-workers investigated Th(IV)−, U(IV)−, U(VI)−, and Np(IV)−sulfate systems under ambient conditions and found that the proportion of monodentate/bidentate linkages was a function of $[SO_4^{2-}]:[An^{n+}]$ ratio.[11] Sulfate coordination and the fraction of bidentate linkages were found to increase with increasing sulfate concentration. Our results are consistent with this finding. As reported here, the solid state structure of **1** was synthesized at a $[SO_4^{2-}]:[Th^{4+}]$ ratio = 1 and it contains only monodentate linkages. At $[SO_4^{2-}]:[Th^{4+}]$ ratio > 8, as reported by Hennig, monodentate and bidentate coordination is observed in solution.[11]

Metrical analysis of a HEXS pattern obtained from a solution from which compound **1** crystallizes provide information that may guide directed syntheses of Th sulfate compounds. For comparison, in the solid-state structure of **1** Th is also nine coordinate, bound to the oxygen atoms from two monodentate sulfate units, instead of the one seen in solution, and seven bound water molecules, with average bond lengths of 2.379 and 2.468 Å, respectively . The solution PDF data do not show any splitting of the first coordination sphere oxygen atoms between those arising from sulfate and those of water, likely the result of the data resolution and not from distance averaging in solution. A similar result was observed in the trigonal bipyramidal coordination of Cm^{3+}, which has a subshell splitting of 0.092(2) Å determined from the crystal structure. Solution HEXS data were unable to resolve the two subshell aqua coordination about the Cm^{3+}, whereas EXAFS data from the same solution were able to do so but only when including data out to very large k $(Å)^{-1}$. Similar to the Th work herein, the HEXS distance obtained from the *Cm* solution agreed with the weighted average from the solid-state structure.[36]

The HEXS data suggest a polynuclear thorium complex in solution where the two thorium centers are bridged by a monodentate sulfate anion. This type of bridging motif is common to the solid state structures of the heavier tetravalent actinides U to Pu,[39−41] Zr,[42] and Ce(IV)[43] of the formula $M(SO_4)_2(H_2O)_4$. However, an isostructural complex of Th has yet to be reported, perhaps indicating a break in what one would expect to be a periodic structural family. Additionally, the evidence from the PDF of solution HEXS data of more distant Th correlations at about 5.9(2) Å is particularly interesting and suggests intermediate-range organization prior to crystallization. Such behavior has been previously reported in aqueous solutions from which hydroxo-

dx.doi.org/10.1021/ic201175u |*Inorg. Chem.* 2011, 50, 8621–8629

bridged Th complexes precipitate.[44] Although the thermodynamic stability constants for both Th sulfate and bis(sulfate) are fairly large (log K approximately 4 and 8, respectively),[6,45] thus indicating strong complexation, it is not possible to assume anything about inner- versus outer-sphere sulfate from these values, as has been recently demonstrated by HEXS studies of metal ion correlations in solution.[35,37] Following this precedent, a similar study of Th sulfate correlations in solution as a function of sulfate ion concentration, when compared with known stability constants, may provide more detailed information to complement both the work described herein and previously published EXAFS studies.[11]

Interestingly, **2** and **3** contain exclusively monodentate sulfate units despite having been synthesized at much higher $[SO_4^{2-}]$:$[Th^{4+}]$ ratios than **1**. Unlike **1**, however, **2** and **3** were synthesized with heating or under hydrothermal conditions raising the prospect that temperature plays a role in product formation. Bidentate chelation of the Th(IV) centers by the sulfate anion requires the dissociation of the bisulfate anion (HSO_4^-). Temperature is known to impact the properties of solvent water, specifically the dielectric constant for water decreases with increasing temperature. As such electrolytes that are completely dissociated under ambient conditions tend to associate with rising solvent temperature. The dissociation of HSO_4^- ($pK_a \sim 2$) is temperature dependent and the degree of dissociation for bisulfate has been found to decrease with increasing temperature.[46] This would suggest a predominance of monodentate HSO_4^- linkages but instead monodentate SO_4^{2-} units are observed in the crystal structures of the reported compounds.

Monodentate SO_4^{2-} units formed under acidic conditions, below the pK_a of HSO_4^-, are also present in the architecture of $Na_2[Th(SO_4)_3(H_2O)_3]\cdot 3H_2O$.[16] Moreover, the metal−sulfate coordination mode found in this material cannot be explained by either $[SO_4^{2-}]$:$[Th^{4+}]$ ratios or temperature considerations. The compound reported by Habash and Smith was synthesized at room temperature at $[SO_4^{2-}]$:$[Th^{4+}]$ ratios greater than 1 yet the structure is built from nine-coordinate Th^{4+} centers bound to six monodentate sulfate groups and three water molecules. Such examples indicate that variables other than pH, temperature, and reactant ratios play a definitive role in product formation. Undoubtedly, relative solubilities play a role in crystal formation, which may not be representative of relative solution speciation. The structures may also suggest that the ability of the metal ion to stabilize bisulfate versus sulfate contributes to the coordination mode of the sulfate unit. If such were the case, we would expect that the prevalence of monodentate versus chelating bidentate coordination would decrease with increasing charge density of the metal ion and more polarizing metal cations would be more likely to stabilize the SO_4^{2-} anion below its pK_a. Hennig et al. examined aqueous An(IV) sulfate systems under comparable conditions using EXAFS and found that the spectrum of Th(IV) sulfate exhibited larger FT peaks from monodentate sulfate as compared to that of U(IV).[11] Moreover, comparison of the EXAFS FT of Th(IV), U(IV), and Np(IV) sulfate solutions showed an increase in bidentate sulfate coordination along the series Th(IV)−U(IV)−Np(IV).[9] Such a trend is not entirely discernible upon examination of reported An(IV) solid state structures, however, and thus warrants continued investigation.

CONCLUSIONS

The syntheses a characterization of three thorium sulfates, $Th(SO_4)_2(H_2O)_7\cdot 2(H_2O)$, $Th_4(SO_4)_7(H_2O)_7(OH)_2\cdot H_2O$, and $Th(OH)_2SO_4$, have been described. In **1**−**3**, the sulfate units bind each Th^{4+} metal center exclusively in a monodentate manner. Such coordination has been observed previously in two other Th(IV) sulfates including $Na_2[Th(SO_4)_3(H_2O)_3]\cdot 3H_2O$[16] and $Th_3(SO_4)_6(H_2O)_6$.[20] The structures of the remaining Th^{4+}−SO_4^{2-} compounds contain a combination of monodentate and chelating bidentate sulfate coordination. Factors that likely contribute to the prevalence of monodentate versus bidentate coordination include $[SO_4^{2-}]$:$[Th^{4+}]$ ratios, pH, temperature, and the charge density of the metal cation. However, a general trend that accounts for the metal−sulfate coordination mode observed in all of the reported Th−sulfates crystal structures including those described herein is not yet clear. The coordination behavior of the sulfate anions to Th in solution prior to the crystallization of **1** highlights the difficulty in predicting speciation and it relationship to stability and solubility. In fact, our inability to rationalize or predict the coordination mode of the sulfate unit under various synthetic conditions emphasizes the need to explore such systems with much more depth.

ASSOCIATED CONTENT

Supporting Information. Crystallographic data have also been deposited with the Inorganic Crystal Structure Database (ICSD) and may be obtained at http://icsd.fiz-karlsruhe.de by referencing nos. 422947 (**1**), 422948 (**2**), and 422949 (**3**). ORTEP illustrations, powder diffraction data, IR and Raman spectra. This material is available free of charge via the Internet at http://pubs.acs.org.

AUTHOR INFORMATION

Corresponding Author
*E-mail: ls@anl.gov.

ACKNOWLEDGMENT

This work was performed at Argonne National Laboratory, operated by UChicagoArgonne LLC for the United States Department of Energy under contract number DE-AC02-06CH11357 and was supported by a DOE Office of Basic Energy Sciences, Chemical Sciences Heavy Elements Chemistry. The work at the APS was supported by the Office of Basic Energy Sciences, Scientific User Facilities, under the same contract number.

REFERENCES

(1) Seaborg, G. T. *Nucleonics* **1949**, *5*, 16–36.
(2) Seaborg, G. T. Electronic structure of the heaviest elements. In *NNES PPR, Vol. 14B, The Transuranium Elements: Research Papers*; McGraw-Hill Book Co., Inc.: New York, 1949; p Paper No. 21.1.
(3) Silva, R. J.; Nitsche, H. *Radiochim. Acta* **1995**, *70*−*1*, 377–396.
(4) Zachariasen, W. *Acta Crystallogr.* **1949**, *2*, 388–390.
(5) Sellers, P. A.; Fried, S.; Elson, R. E.; Zachariasen, W. H. *J. Am. Chem. Soc.* **1954**, *76*, 5935–5938.
(6) Rand, M.; Fuger, J.; Grenthe, I.; Neck, V.; Rai, D. *Chemical Thermodynamics of Thorium*; OECD Publishing; 2008.
(7) Grenthe, I.; Fuger, J.; Konings, R. J. M.; Lemire, R. J.; Muller, A. B.; Cregu, C. N.-T.; Wanner, H. *Chemical Thermodynamics of Uranium*; OECD Publishing; 2004.
(8) Lemire, R. J.; Fuger, J.; Nitsche, H.; Potter, P.; Rand, M. H.; Rydberg, J.; Spahiu, K.; Sullivan, J. C.; Ullman, W. J.; Vitorge, P.; Wanner, H., *Chemical thermodynamics of Neptunium and Plutonium*; Elsevier: Amsterdam; 2001.

(9) Hennig, C.; Ikeda-Ohno, A.; Tsushima, S.; Scheinost, A. C. *Inorg. Chem.* **2009**, *48*, 5350–5360.
(10) Hennig, C.; Kraus, W.; Emmerling, F.; Ikeda, A.; Scheinost, A. C. *Inorg. Chem.* **2008**, *47*, 1634–1638.
(11) Hennig, C.; Schmeide, K.; Brendler, V.; Moll, H.; Tsushima, S.; Scheinost, A. C. *Inorg. Chem.* **2007**, *46*, 5882–5892.
(12) Wilson, R. E. *Inorg. Chem.* **2011**, *50*, 5663–5670.
(13) Arutyunyan, E. G.; Porai-Koshits, M. A.; Molodkin, A. M. *J. Struct. Chem.* **1966**, *7*, 683–686.
(14) Habash, J.; Beddoes, R. L.; Smith, A. J. *Acta Crystallogr., Sect. C* **1991**, *47*, 1595–1597.
(15) Habash, J.; Smith, A. J. *Acta Crystallogr., Sect. C* **1983**, *39*, 413–415.
(16) Habash, J.; Smith, A. J. *Acta Crystallogr., Sect. C* **1990**, *46*, 957–960.
(17) Habash, J.; Smith, A. J. *J. Crystallogr. Spectrosc. Res.* **1992**, *22*, 21–24.
(18) Behera, J. N.; Rao, C. N. R. *Z. Anorg. Allg. Chem.* **2005**, *631*, 3030–3036.
(19) Lundgren, G. *Arkiv for Kemi* **1950**, *2*, 535–549.
(20) Wilson, R. E.; Skanthakumar, S.; Knope, K. E.; Cahill, C. L.; Soderholm, L. *Inorg. Chem.* **2008**, *47*, 9321–9326.
(21) Lundgren, G. *Arkiv for Kemi* **1952**, *2*, 421–428.
(22) Wester, D. W.; Mulak, J.; Banks, R.; Carnall, W. T. *J. Solid State Chem.* **1982**, *45*, 235–240.
(23) Shannon, R. D. *Acta Crystallogr., Sect. A* **1976**, *32*, 751.
(24) Wilson, R. E.; Skanthakumar, S.; Burns, P. C.; Soderholm, L. *Angew. Chem., Int. Ed.* **2007**, *46*, 8043–8045.
(25) Albrecht, A. J.; Sigmon, G. E.; Moore-Shay, L.; Wei, R.; Dawes, C.; Szymanowski, J.; Burns, P. C. *J. Solid State Chem.* **2011**, *184*, 1591–1597.
(26) *Bruker APEX2 Software Suite*, APEX2 v2010.7−0; Bruker AXS: Madison, WI, 2010.
(27) Sheldrick, G. M. *Acta Crystallogr.* **2008**, *A64*, 112–122.
(28) Spek, A. L. *Acta Crystallogr., Sect. A* **1990**, *46*, C34.
(29) Brese, N. E.; O'Keefe, M. *Acta Crystallogr.* **1991**, *B47*, 192.
(30) Toby, B. H. *J. Appl. Crystallogr.* **2001**, *34*, 210–213.
(31) Larson, A. C.; Von Dreele, R. B. *Los Alamos National Laboratory Report LAUR 86−748* **1994**.
(32) Skanthakumar, S.; Soderholm, L. *Mater. Res. Soc. Symp. Proc.* **2006**, *893*, 411–416.
(33) Soderholm, L.; Skanthakumar, S.; Neuefeind, J. *Anal. Bioanal. Chem.* **2005**, *383*, 48–55.
(34) Nakamoto, K., *Infrared and Raman Spectra of Inorganic and Coordination Compounds Part B: Applications in Coordination, Oragnometallic, and Bioinorganic Chemistry*, Fifth ed.; John Wiley & Sons, Inc.: New York; 1997.
(35) Soderholm, L.; Skanthakumar, S.; Wilson, R. E. *J. Phys. Chem. A* **2011**, *115*, 4959–4967.
(36) Skanthakumar, S.; Antonio, M. R.; Wilson, R. E.; Soderholm, L. *Inorg. Chem.* **2007**, *46*, 3485–3491.
(37) Soderholm, L.; Skanthakumar, S.; Wilson, R. E. *J. Phys. Chem. A* **2009**, *113*, 6391–6397.
(38) Wilson, R. E.; Skanthakumar, S.; Soderholm, L. *Mater. Res. Soc. Symp. Proc.* **2007**, *986*, 183–188.
(39) Kierkegaard, P. *Acta Chem. Scand.* **1956**, *10*, 599–616.
(40) Jayadevan, N. C.; Mudher, K. D. S.; Chackraburtty, D. M. *Z. Kristallogr.* **1982**, *161*, 7–13.
(41) Charushnikova, I. A.; Krot, N. N.; Starikova, Z. A. *Radiochemistry* **2000**, *42*, 434–438.
(42) Singer, J.; Cromer, D. T. *Acta Crystallogr.* **1959**, *12*, 719–723.
(43) Casari, B. M.; Langer, V. *J. Solid State Chem.* **2007**, *180*, 1616–1622.
(44) Wilson, R. E.; Skanthakumar, S.; Sigmon, G.; Burns, P. C.; Soderholm, L. *Inorg. Chem.* **2007**, *46*, 2368–2372.
(45) Langmuir, D.; Herman, J. S. *Geochim. Cosmochim. Acta* **1980**, *44*, 1753–1766.
(46) Knopf, D. A.; Luo, B. P.; Krieger, U. K.; Koop, T. *J. Phys. Chem. A* **2003**, *107*, 4322–4332.